Polar Meteorol. Glaciol., **13**, 148-156, 1999

Report

SNOW PARTICLE SIZE DISTRIBUTIONS AT SYOWA STATION, ANTARCTICA IN 1988

Masahiko HATANAKA[1], Shinya KIMURA[1], Yutaka YOSHIDA[1], Makoto WADA[2] and Naohiko HIRASAWA[2]

[1] *Muroran Institute of Technology, 27-1, Mizumoto-cho, Muroran 050-8585*
[2] *National Institute of Polar Research, Kaga 1-chome, Itabashi-ku, Tokyo 173-8515*

Abstract: For meteorological radar observations, it is very important to know the size and the characteristics of precipitation particles. In this paper, we report the snow particle size distributions at Syowa Station, Antarctica in 1988 using snow particle VCR tapes, which were recorded by a specially designed portable video camera set on the ground. The digitized video images retrieved from the VCR tape are processed to separate each snow particle on the image. We measured the three kinds of snow particle "radius" on the separated snow particle image and obtained the snow particle size distributions. Using the five sets of VCR tapes, we obtained four cases of distributions at Syowa Station in 1988 and estimated a case of snowfall rate from the distribution.

1. Introduction

The snow particle size distribution is important in the snowfall radar observations (SKOLINIK, 1980). Recently, MURAMOTO *et al.* (1992, 1995) reported a method to measure the size and velocity of falling snowflakes precisely by using two video cameras, and obtained the size distribution and the relationship between the falling velocity and the diameter in Japan. At Syowa Station, Antarctica, KONISHI *et al.* (1990) reported the snow particle sizes and falling velocity distribution obtained by a video camera system in 1989.

Another observation of falling snow particles using by a specially designed portable video camera set was carried out at Syowa Station in 1988, and the relative numbers of snow particles and the shape of their size distribution were obtained from the video cassette recorder (VCR) tapes (HATANAKA *et al.*, 1995). Using this shape of the distribution and the observed meteorological radar echo data at Syowa Station in 1988 (WADA, 1990), TAKEYA *et al.* (1994) tried to calculate snowfall rates based on the fundamental radar equation and showed their results agreed with snowfall rates evaluated from the radar reflectivity factor-snowfall rate (Z-R) relation observed in 1989 (KONISHI *et al.*, 1992). In this work, TAKEYA *et al.* (1994) used the maximum distance between the geometrical center of gravity and periphery for "radius" of snow particle to calculate radar reflectivity coefficient, instead of the conventional equivalent-radius.

In this paper, we quantitatively obtained the three kinds of snow particle size distributions, which are based on r_MAX: the maximum distance between the geometrical center of gravity and periphery, r_area: conventional equivalent radius calculated from the area, and r_max: half of the maximum distance between peripheral points through the geometrical center of gravity using the same VCR tapes for the radar reflectivity coefficient calculation.

2. Method

Snow falling on the ground was observed by the portable video camera set shown in Fig. 1 (HATANAKA *et al.*, 1995). Snow particles fall on the 35 mm width transparent film through the aperture window (24 mm(W) $\times$ 32 mm(L)), and the particle images are recoded on VCR tape. The transparent film is advanced intermittently by a variable time switch and snow particles are accumulated on this film while it is stationary. The typical advancing period and accumulation time were 90 s and 80 s, respectively.

The image on the VCR tape is digitized into 640 $\times$ 400 pixels every 5 sec using a personal computer, but the available image size is 640 $\times$ 350 pixels, excluding the time stamp area (Fig. 2). To distinguish the falling snow particles in a short interval from the accumulated particles on the film and to reduce the background offset level on the image, image subtraction between subsequent digitized images is used. In case of daytime VCR images (see Fig. 2b), the subtracted image is sign-reversed (HATANAKA *et al.*, 1995). To reduce random noise on this subtracted image, a 3 $\times$ 3 median filter (ROSENFELD and KAK, 1981a) is applied, and finally the image is binarized by a threshold. The typical threshold value was 6 (=2% of 256 gray level). To separate each snow particle on the image, the raster tracking method (ROSENFELD and KAK, 1981b) is used. In this processing, a particle touching the boundary of the image is ignored (Fig. 3). If we assume that snow particles fall randomly, the maximum number of snow particles $n_{+}(r)$ is calculated from actually counted number of particles $n(r)$ using by the following equation.

$$n_{+}(r) = 640*350/[(640-2r)\ (350-2r)]*n(r). \qquad (1)$$

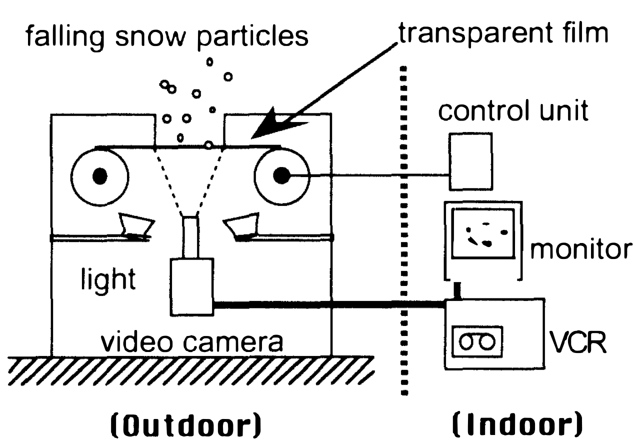

Fig. 1. Configuration of the portable video camera set.

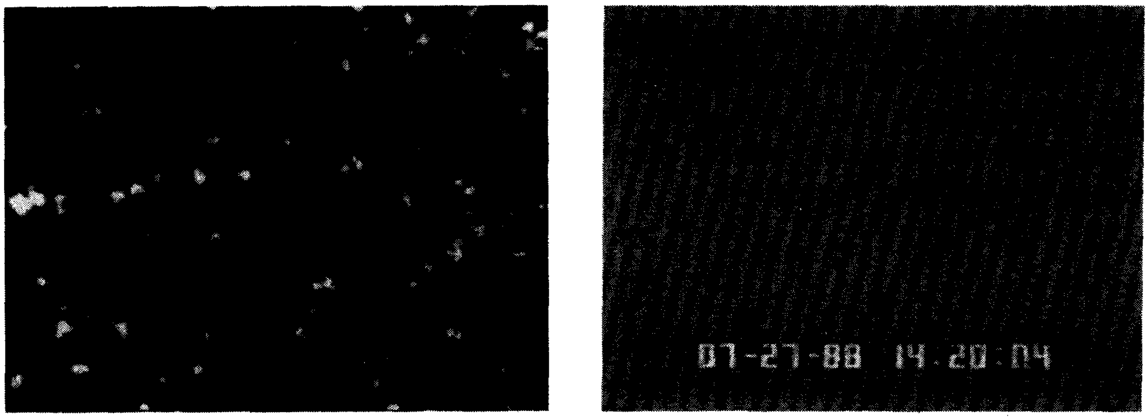

(a) Observed at night. (b) Observed in the daytime.

Fig. 2. Examples of digitized image.

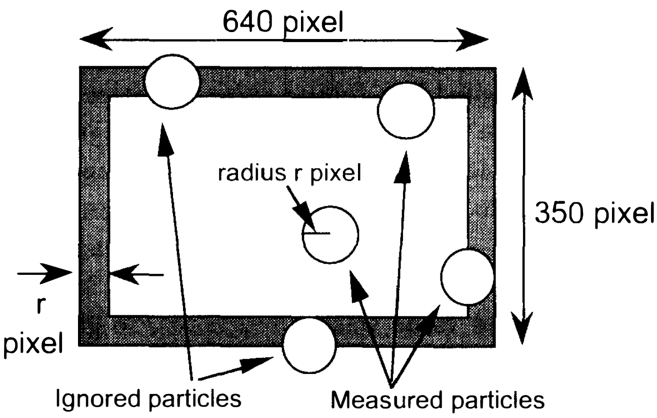

Fig. 3. Ignored snow particles near the image boundary.

We consider that the true measured value is between $n_+(r)$ and $n(r)$.

Three kinds of snow particle "radius" are measured; r_Max: the maximum distance between the geometrical center of gravity and periphery on the particle image; r_max: half of the maximum distance between peripheral points through the center of gravity; and r_area: the equivalent radius calculated from the area. Particles are classified in size ranges per 0.005 cm radius. Snow particle size distributions $N(r)$ and $N_+(r)$ particles/(m^2 hour), obtained from $n(r)$ and $n_+(r)$, respectively, are approximated by the following equation (TAKEYA et al., 1994; HATANAKA et al., 1995).

$$N(r) = A * 10^{-B*r}, \qquad (2)$$

where r is the snow particle radius(r_Max, r_max, r_area), A is a parameter determined by snowfall rate and B is a parameter to determine the shape of the distribution.

Precipitation rate P mm/h is evaluated from the density of snow particles ρ_s and the equivalent radius snow particle size distribution N(r_area).

$$P=\Sigma\rho_s*(3/4)\pi\ r\_area^3*N(r\_area). \tag{3}$$

We used five VCR tapes recorded at Syowa Station, Antarctica in 1988. Their observation periods and some meteorological conditions are summarized in Table 1.

Table 1. Data sheet for the five VCR tapes.

Tape No.	Observation period	Surface air temperature	Surface humidity	Comment
Tape a	21:13, Apr. 5 – 01:33, Apr. 6	-10 ℃	83 %	Graupels
Tape b	14:14, Jul. 27 – 24:00, Jul. 27	-16 ℃	54 %	
Tape c	23:58, Sep. 5 – 02:16, Sep. 6	-21 ℃	55 %	
Tape d	16:11, Sep. 6 – 17:12, Sep. 6	-19 ℃	65 %	
Tape e	18:00, Oct. 1 – 19:44, Oct. 1	-13 ℃	73 %	Aggregates of bullets

3. Results

Three examples of measured snow particle size distributions $N(r)$ and their approximate expressions (2) are shown in Fig. 4. In curve-fitting based on eq. (2), we ignored data in the size range where the radius is less than 0.02 cm and in the range where the number of counted particles is less than 3/4 of the maximum number in this distribution "AND" 10. On both ends of the available range, the number ratio of snow particles was approximately equal to the volume ratio of the snow particles $((8/2)^3=64)$. The snow particles in Fig. 4a, suspected graupels from the VCR images on tape a, were mainly distributed up to 0.07 cm in three "radii". The particles in Fig. 4c, suspected aggregates of bullets from tape e, were distributed up to 0.07 cm in r_MAX and r_max, but limited to 0.03 cm in r_area. This means that the shapes of the particles in the latter case differ considerably from the spherical and the difference of B values between r_MAX and r_area in Fig. 4c was much larger than in Fig. 4a. The measured snow particles on tapes b, c and d were mainly distributed up to 0.08 cm in r_MAX and r_max, but limited to 0.05 in r_area, respectively.

An example of the difference between distributions $N(r)$ and $N_+(r)$ is shown in Fig. 5. In this figure, the lower limit bar shows the value of $N(r\_area)$ and the upper one shows that of $N_+(r\_area)$. Since the difference between $N_+(r)$ to $N(r)$ is widening at the larger radius range in Fig. 5, the parameter B of $N_+(r)$ becomes slightly smaller than that of $N(r)$.

The obtained approximated distribution (represented by parameters A, B) and the number of actually counted particles $\Sigma_r\ n(r)$ are listed in Table 2. In Table 2, the values of parameter B in the last row are calculated from all counted particles on the tape. This result shows that not only the number of fallen snow particles ($\Sigma_r\ n(r)$ or parameter A) but the shape of distribution (parameter B) are changed rapidly. The time variations of parameter B were beyond 10%, and the differences of B parameters between $N(r)$ and $N_+(r)$ were much less than 1%.

(a)

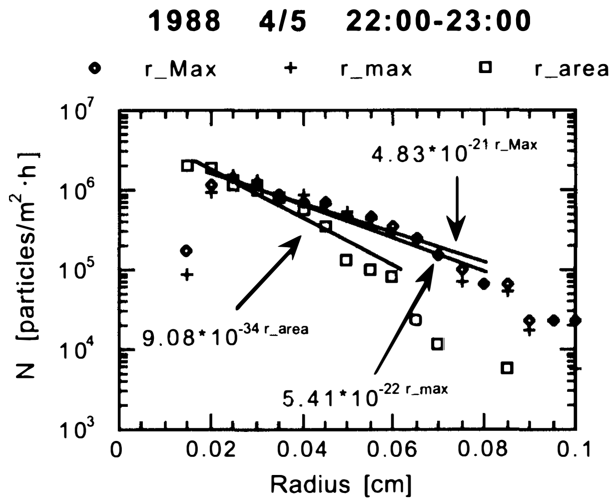

(b)

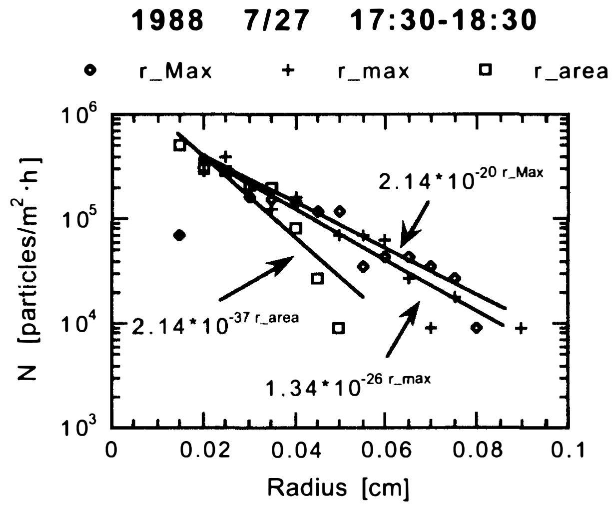

(c)

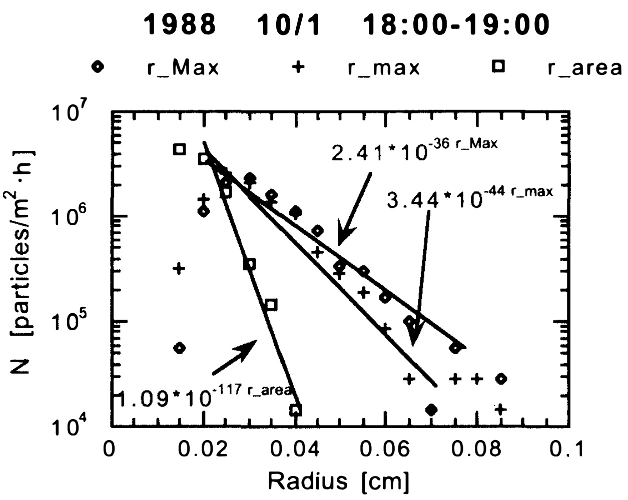

Fig. 4. Examples of measured snow particle size distributions at Syowa Station, Antarctica in 1988. (a) Tape a: from 2200 LT to 2300 LT on April 5, (b) tape b: from 1730 LT to 1830 LT on July 27, and (c) tape e: from 1800 LT to 1900 LT on October 1.

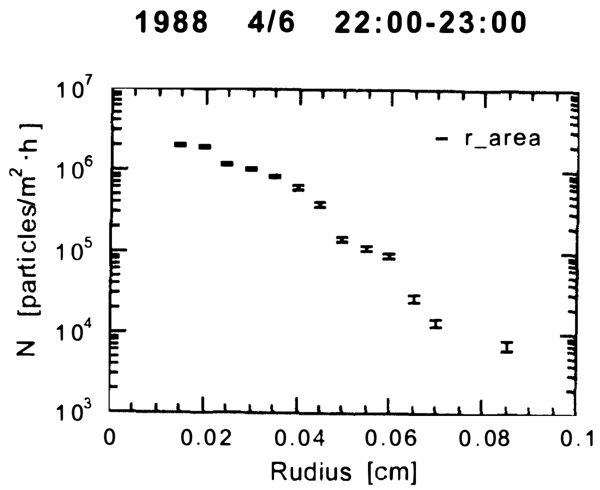

Fig. 5. An example of N(r) and $N_+(r)$: the lower limit bar shows N(r_area) and the upper one shows N_+(r_area).

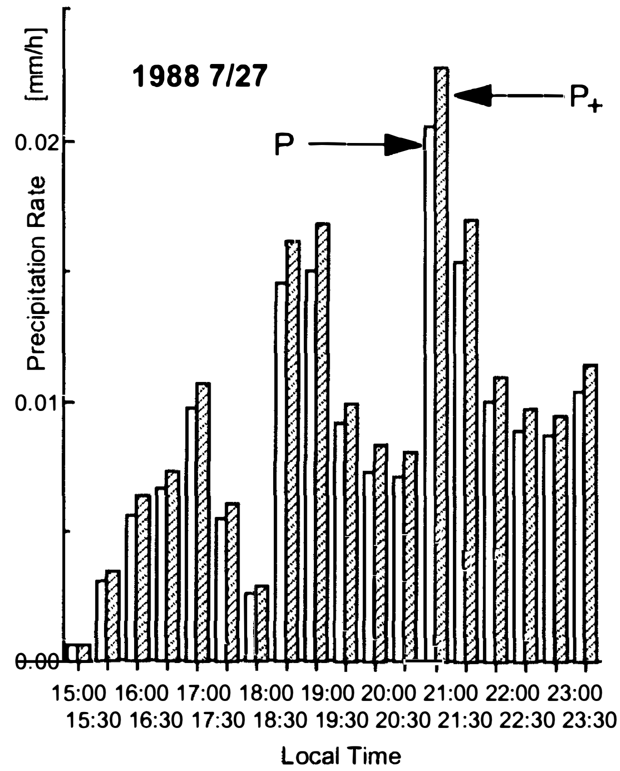

Fig. 6. An example of precipitation rates P and P_+.

An example of the precipitation rates P and P_+ mm/h estimated from the $N(r\_area)$ and $N_+(r\_area)$ are shown in Fig. 6. In this estimation, we assumed that the density of snow particles ρ_s can be calculated from the volume content of water p_w ($p_w \approx \rho_s^2$; NISHITSUJI, 1971) and the calculated value of ρ_s is 0.021 g/cm^3 (TAKEYA *et al.*, 1994). In Fig. 6, the maximum difference between P and P_+ is 13.5% and the averaged difference is about 10%.

Table 2. Obtained parameters A and B in eq. (2).

Tape a (Apr. 05)	Σ_r n(r)	Parameter A / parameter B					
		N(r_MAX)	N_+(r_MAX)	N(r_max)	N_+(r_max)	N(r_area)	N_+(r_area)
21:13-22:00	221	$1.20*10^{6}$ / 20	$1.20*10^{6}$ / 19	$1.07*10^{6}$ / 18	$1.07*10^{6}$ / 17	$1.79*10^{6}$ / 27	$1.79*10^{6}$ / 26
21:30-22:30	1184	$4.18*10^{6}$ / 20	$4.17*10^{6}$ / 19	$4.96*10^{6}$ / 22	$4.93*10^{6}$ / 21	$1.61*10^{7}$ / 41	$1.61*10^{7}$ / 40
22:00-23:00	1421	$4.83*10^{6}$ / 21	$4.81*10^{6}$ / 20	$5.41*10^{6}$ / 22	$5.38*10^{6}$ / 21	$9.08*10^{6}$ / 34	$9.06*10^{6}$ / 33
22:30-23:30	604	$2.69*10^{6}$ / 24	$2.67*10^{6}$ / 23	$3.88*10^{6}$ / 28	$3.87*10^{6}$ / 27	$1.87*10^{7}$ / 55	$1.86*10^{7}$ / 54
23:00-00:00	703	$3.68*10^{6}$ / 24	$3.67*10^{6}$ / 23	$4.22*10^{6}$ / 26	$4.20*10^{6}$ / 25	$1.30*10^{7}$ / 48	$1.30*10^{7}$ / 47
23:30-00:30	2819	$1.26*10^{7}$ / 21	$1.26*10^{7}$ / 20	$1.61*10^{7}$ / 24	$1.60*10^{7}$ / 23	$6.82*10^{7}$ / 46	$6.79*10^{7}$ / 45
00:00-01:00	5861	$2.34*10^{7}$ / 23	$2.33*10^{7}$ / 22	$3.08*10^{7}$ / 27	$3.06*10^{7}$ / 25	$6.22*10^{7}$ / 42	$6.21*10^{7}$ / 41
00:30-01:30	5805	$2.83*10^{7}$ / 28	$2.82*10^{7}$ / 26	$3.41*10^{7}$ / 30	$3.40*10^{7}$ / 28	$1.21*10^{8}$ / 52	$1.21*10^{8}$ / 51
21:13-01:30	----	------- / 24	------- / --	------- / 27	------- / --	------- / 48	------- / --

Tape b (Jul. 27)	Σ_r n(r)	Parameter A / parameter B					
		N(r_MAX)	N_+(r_MAX)	N(r_max)	N_+(r_max)	N(r_area)	N_+(r_area)
14:14-15:00	198	$2.19*10^{7}$ / 59	$2.19*10^{7}$ / 59	$2.47*10^{7}$ / 63	$2.47*10^{7}$ / 62	$3.15*10^{7}$ / 99	$3.15*10^{7}$ / 97
14:30-15:30	125	$6.86*10^{5}$ / 28	$6.83*10^{5}$ / 26	$1.05*10^{6}$ / 34	$1.04*10^{6}$ / 32	$1.69*10^{6}$ / 48	$1.68*10^{6}$ / 47
15:00-16:00	242	$1.82*10^{6}$ / 28	$1.82*10^{6}$ / 26	$2.34*10^{6}$ / 30	$2.33*10^{6}$ / 29	$6.20*10^{6}$ / 54	$6.19*10^{6}$ / 53
15:30-16:30	211	$3.04*10^{6}$ / 29	$3.03*10^{6}$ / 27	$3.01*10^{6}$ / 28	$3.00*10^{6}$ / 27	$3.43*10^{6}$ / 36	$3.42*10^{6}$ / 35
16:00-17:00	228	$3.91*10^{6}$ / 29	$3.89*10^{6}$ / 27	$3.33*10^{6}$ / 27	$3.31*10^{6}$ / 25	$4.09*10^{6}$ / 34	$4.08*10^{6}$ / 32
16:30-17:30	550	$6.05*10^{6}$ / 29	$6.02*10^{6}$ / 27	$9.94*10^{6}$ / 34	$9.89*10^{6}$ / 33	$1.06*10^{7}$ / 49	$1.06*10^{7}$ / 48
17:00-18:00	558	$3.04*10^{6}$ / 26	$3.03*10^{6}$ / 25	$4.47*10^{6}$ / 31	$4.45*10^{6}$ / 29	$8.28*10^{6}$ / 48	$8.27*10^{6}$ / 46
17:30-18:30	182	$8.37*10^{5}$ / 20	$8.34*10^{5}$ / 19	$1.34*10^{6}$ / 26	$1.33*10^{6}$ / 25	$2.14*10^{6}$ / 37	$2.14*10^{6}$ / 36
18:00-19:00	228	$4.28*10^{6}$ / 23	$4.26*10^{6}$ / 22	$5.12*10^{6}$ / 26	$5.10*10^{6}$ / 24	$4.57*10^{6}$ / 27	$4.55*10^{6}$ / 26
18:30-19:30	211	$4.29*10^{6}$ / 23	$4.27*10^{6}$ / 22	$8.79*10^{6}$ / 29	$8.74*10^{6}$ / 28	$1.51*10^{7}$ / 43	$1.50*10^{7}$ / 42
19:00-20:00	25	$1.08*10^{6}$ / 03	$1.08*10^{6}$ / 02	$1.49*10^{6}$ / 07	$1.49*10^{6}$ / 06	$6.89*10^{6}$ / 27	$6.86*10^{6}$ / 25
19:30-20:30	121	$1.42*10^{6}$ / 20	$1.41*10^{6}$ / 19	$2.03*10^{6}$ / 24	$2.03*10^{6}$ / 23	$2.15*10^{6}$ / 29	$2.15*10^{6}$ / 27
20:00-21:00	98	$2.26*10^{6}$ / 27	$2.25*10^{6}$ / 26	$2.54*10^{6}$ / 28	$2.53*10^{6}$ / 27	$3.46*10^{6}$ / 37	$3.45*10^{6}$ / 36
20:30-21:30	373	$7.94*10^{6}$ / 25	$7.90*10^{6}$ / 24	$1.17*10^{7}$ / 29	$1.16*10^{7}$ / 28	$1.17*10^{7}$ / 35	$1.17*10^{7}$ / 34
21:00-22:00	613	$7.42*10^{6}$ / 26	$7.39*10^{6}$ / 23	$1.39*10^{7}$ / 34	$1.38*10^{7}$ / 32	$2.68*10^{7}$ / 48	$2.67*10^{7}$ / 47
21:30-22:30	279	$4.55*10^{6}$ / 22	$4.54*10^{6}$ / 21	$8.42*10^{6}$ / 30	$8.40*10^{6}$ / 29	$1.17*10^{7}$ / 41	$1.17*10^{7}$ / 40
22:00-23:00	60	$8.80*10^{6}$ / 33	$8.79*10^{6}$ / 31	$5.92*10^{6}$ / 28	$5.90*10^{6}$ / 26	$7.96*10^{6}$ / 35	$7.95*10^{6}$ / 34
22:30-23:30	97	$9.89*10^{6}$ / 34	$9.86*10^{6}$ / 33	$8.33*10^{6}$ / 32	$8.31*10^{6}$ / 31	$9.64*10^{6}$ / 38	$9.63*10^{6}$ / 37
23:00-24:00	150	$7.52*10^{6}$ / 29	$7.49*10^{6}$ / 27	$9.44*10^{6}$ / 31	$9.41*10^{6}$ / 30	$1.83*10^{7}$ / 47	$1.82*10^{7}$ / 46
14:14-24:00	----	------- / 28	------- / --	------- / 32	------- / --	------- / 46	------- / --

Table 2. (continued).

Tape c (Sep. 06)	Σ_r n(r)	Parameter A / parameter B					
		N(r_MAX)	N_+(r_MAX)	N(r_max)	N_+(r_max)	N(r_area)	N_+(r_area)
00:00-01:00	619	$2.92*10^7$/45	$2.91*10^7$/44	$2.95*10^7$/48	$2.95*10^7$/44	$6.93*10^8$/111	$6.92*10^8$/110
00:30-01:30	351	$1.12*10^7$/48	$1.12*10^7$/47	$3.05*10^7$/42	$3.03*10^7$/40	$7.18*10^8$/107	$7.17*10^8$/106
01:00-02:00	752	$3.06*10^7$/46	$3.05*10^7$/45	$3.17*10^7$/47	$3.15*10^7$/46	$1.85*10^9$/127	$1.85*10^9$/125
00:00-02:00	----	------- /45	------- /--	------- /46	------- /--	------ /105	------ /---

Tape d (Sep. 06)	Σ_r n(r)	Parameter A / parameter B					
		N(r_MAX)	N_+(r_MAX)	N(r_max)	N_+(r_max)	N(r_area)	N_+(r_area)
16:00-17:00	1444	$2.33*10^7$/34	$2.32*10^7$/33	$4.00*10^7$/41	$3.99*10^7$/40	$1.97*10^8$/80	$1.96*10^8$/78

Tape e (Oct. 01)	Σ_r n(r)	Parameter A / parameter B					
		N(r_MAX)	N_+(r_MAX)	N(r_max)	N_+(r_max)	N(r_area)	N_+(r_area)
18:00-19:00	708	$2.41*10^7$/36	$2.40*10^7$/34	$3.44*10^7$/44	$3.43*10^7$/43	$1.09*10^9$/117	$1.08*10^9$/116
18:30-19:30	705	$3.21*10^7$/39	$3.20*10^7$/38	$3.08*10^7$/45	$3.07*10^7$/44	$5.70*10^8$/122	$5.69*10^8$/120
18:00-19:30	----	------- /31	------- /--	------- /40	------- /--	------ /130	------ /---

4. Discussion and Summary

Three kinds of snow particle size distributions at Syowa Station, Antarctica on April 5, July 27, September 6 and October 1 in 1988 were obtained from the snow falling VCR tapes, and a series of precipitation rates on July 27 was evaluated from the obtained distribution.

TAKEYA *et al.* (1994) showed that calculated snowfall rate from the radar data in 1988 and the radar equation agreed with the result evaluated from the Z-R relation based on the observations in 1989 (KONISHI *et al.*, 1992). Since they adopted *r*_MAX for "radius" of snow particle for the distribution, there is a possibility that the "radius" of non-spherical snow particle for radar reflection is larger than the conventional equivalent radius *r*_area. To clear this possibility, we need to obtained distributions based on various kinds of "radius" for calculating the radar reflectivity coefficient and snowfall rate in the same snowfall, at first. Unfortunately there is not directly observed snowfall rate data in 1988 data set, we tried to evaluate snowfall rate using VCR tape. That is the reason why we used not only *r*_area but other kinds of "radius"(*r*_MAX, *r*_max) to obtained short-term snow particle size distribution. We think that *r*_MAX might be over estimated "radius" and *r*_max is one of the "radius" which value lies between *r*_MAX and *r*_area.

Among the obtained distributions *N*(*r*_MAX), *N*(*r*_max) and *N*(*r*_area) in Fig. 4, there were large differences between *N*(*r*_area) and other two distributions. Sometimes, the values of the parameter *B* on *N*(*r*_area) were two times as large as those of other two distributions in Table 2. The time variations of parameter *B* were 10–50% and the differences of parameter *B* between $N(r)$ and $N_+(r)$ were much less than 1%.

To test the availability of the non-spherical snow particle "radius" r_MAX and r_max for radar reflection, we will re-calculate the snowfall rate using the observed radar echo data in 1988 and the normalized distributions $N_0(r\_MAX)$, $N_0(r\_max)$, $N_0(r\_area)$ in Table 2, and compare these results to the snowfall rate shown in Fig. 6.

References

HATANAKA, M., OHTA, Y., NISHITSUJI, A., SAKAGUCHI, T. and WADA, M. (1995): A method of measuring snow particle size from video images for meteorological radar observations. Proc. NIPR Symp. Polar Meteorol. Glaciol., **9**, 110–117.

HATANAKA, M., TAKEYA, H., KIMURA, S., YOSHIDA, Y., NISHITSUJI, A., WADA, M. and HIRASAWA, N. (1997): Kishô rêdâ ekô kara motometa kôsetsu kyôdo no hyôka ni tsuite (An evaluation of snowfall rate estimated from meteorological radar data). Technical Rep. IEICE, **EMCJ97-44**, 67–73.

KONISHI, H., MURAMOTO, K., SHIINA, T., ENDOH, T. and KITANO, K. (1990): Syôwa Kichi ni okeru kôsetsu ryûshi kansoku. 13th Symp. Polar Meteorol. Glaciol. Programme & Abstracts., 92.

KONISHI, H., MURAMOTO, K., SHIINA, T., ENDOH, T. and KITANO, K. (1992): Z-R relation for graupels and aggregates observed at Syowa Station, Antractica. Proc. NIPR Symp. Polar Meteorol. Glaciol., **5**, 97–103.

MURAMOTO, K., MATSUURA, K., SHIINA, T., ENDOH, T. and KONISHI, H. (1992): Measurement of falling motion of snowflakes using CCD camera. Proc. NIPR Symp. Polar Meteorol. Glaciol., **6**, 71–76.

MURAMOTO, K., TAKAGI, S., SHIINA, T. and MATSUURA, K. (1995): 2-dai no kamera wo tsukatta kôsetsu ryûshi no keijyô to rakka sokudo no dôji sokutei (Simultaneous measurement of shape and fall velocity of snow particles using two cameras). IEICE Trans., **J78-D-II** (8), 1249–1253.

NISHITSUJI, A. (1971): Method of calculation of radio-wave attenuation in snowfall. Electron. Commun. Jpn., **54** (1), 74–81.

ROSENFELD, A. and KAK, A.C. (1981a): Digital Picture Processing, 2nd ed., **1**, New York, Academic Press, 261–264.

ROSENFELD, A. and KAK, A.C. (1981b): Digital Picture Processing, 2nd ed., **2**, New York, Academic Press, 130–133, 139–140.

SKOLNIK, M.I. (1980): Introduction to Radar Systems, 2nd ed. Singapore, McGraw-Hill International Editions, 498–503.

TAKEYA, H., HATANAKA, M., SAKAGUCHI, T., NISHITSUJI, A., HOSHIYAMA, M. and WADA, M. (1994): A method to analyze the meteorological radar echo observed at Syowa Station, Antarctica. Proc. NIPR Symp. Polar Meteorol. Glaciol., **8**, 169–177.

WADA, M. (1990): Antarctic climate research data, Part 2. Radar and microwave radiometer data at Syowa Station, Antarctica from March to December 1988. JARE Data Rep., **153** (Meteorology 24), 1–17.

(Received May 6, 1999; Revised manuscript accepted August 18, 1999)